Relaxed SiGe Layers with High Ge Content by Compliant Substrates

H. Yin[1], R.L. Peterson[1], K.D. Hobart[2], S.R. Shieh[3], T.S. Duffy[3], and J.C. Sturm[1]
[1]Center for Photonics and Optoelectronic Materials and Department of Electrical Engineering, Princeton University, Princeton, NJ 08544
[2]Naval Research Laboratory, Washington, DC 20357
[3]Department of Geosciences, Princeton University, Princeton, NJ 08544

ABSTRACT

Relaxed, high Ge content SiGe layers have been realized using stress balance on a compliant borophosphorosilicate glass (BPSG). A 30-nm fully-strained $Si_{0.7}Ge_{0.3}$ layer was transferred onto a 1 μm BPSG film by wafer-bonding and Smart-cut® processes, after which the continuous $Si_{0.7}Ge_{0.3}$ film was patterned into small islands to allow for lateral expansion. After the strain in $Si_{0.7}Ge_{0.3}$ islands was released by the lateral expansion resulting from the flow of the BPSG, a $Si_{0.4}Ge_{0.6}$ layer was commensurately deposited under compression. Upon equilibrium after an annealing, stress balance was formed between the SiGe films, resulting in a larger in-plane lattice constant than that of relaxed $Si_{0.7}Ge_{0.3}$. With a thiner (6 nm) $Si_{0.7}Ge_{0.3}$ starting film, an in-plane lattice constant equivalent to fully-relaxed $Si_{0.45}Ge_{0.55}$ has been obtained.

INTRODUCTION

Relaxed SiGe has recently drawn attention for its wide application in advanced electronics and opto-electronics. The carrier mobility can be considerably enhanced in strained-Si and strained-Ge MOSFETs fabricated on relaxed SiGe [1,2]. It also allows the integration of III-V semiconductors with Si substrates [3]. Conventionally, relaxed SiGe is made by thick compositionally-graded SiGe buffers grown on silicon (~ 1 μm per 10% Ge change). Because of the interaction of misfit dislocations to cause threading dislocations, relaxed SiGe fabricated by this approach suffers from a high density of threading dislocations (about 10^6 cm^{-3}) [4].

The recent application of viscous BPSG as a compliant substrate has yielded high-quality, fully-relaxed $Si_{0.7}Ge_{0.3}$ films through a process which does not fundamentally require misfit dislocations [5,6]. The process is described as follows: a 30-nm $Si_{0.7}Ge_{0.3}$ film commensurately strained to bulk Si(100) is transferred to a 200-nm BPSG film (4.4% B and 4.1% P by weight) on a silicon wafer by wafer-bonding, Smart-cut® and etch-back processes, and then patterned to islands. No relaxation takes place up to this point, since the highest process temperature is 550°C and therefore the BPSG film remains rigid. When the anneal temperature is elevated to 800°C, the BPSG film softens (a viscosity of 1.2 x 10^{11}Poise at 800°C) and the as-bonded, compressively-strained $Si_{0.7}Ge_{0.3}$ film starts to relax by macroscopic expansion. Transmission electron microscopy (TEM) examination has indicated that the dislocation density is low and therefore suggested that the underlying relaxation mechanism is indeed the lateral expansion of SiGe layers on viscous BPSG films when the island dimension is small enough to prevent buckling [6].

Our previous work has shown stress balance in bilayer structures of pseudomorphic silicon grown on thin SiGe and of SiO_2 deposited on thin SiGe before relaxation [7]. Consider two elastic layers on top of a compliant BPSG (Fig. 1). When BPSG turns viscous during a high-temperature annealing (usually at 800°C), the force from the BPSG film, which previously holds

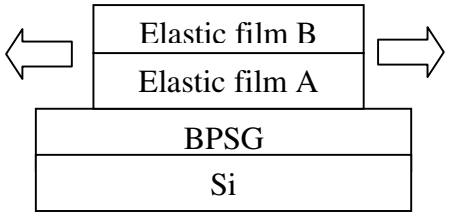

Fig. 1. Schematic of stress balance between elastic films on BPSG. During high-temperature annealing, the BPSG softens and the effectively freestanding elastic films minimize strain energy by lateral displacement. The equilibrium state is governed by net zero stress.

strain in the top bilayer, disappears and as a result, the top films are decoupled from the BPSG and are capable of lateral expansion or shrinkage to lower strain energy. The final strain in the films upon equilibrium is determined to first order by net zero stress in the bilayer:

$$\frac{E_A}{1-\nu_A}\varepsilon_A h_A + \frac{E_B}{1-\nu_B}\varepsilon_B h_B = 0, \quad (1)$$

where E, ν, ε, and h represent the Young's Modulus, Possion's ratio, strain, and the thickness of the film, respectively. In earlier work, tensile Si had been demonstrated when a stack comprising compressively-strained SiGe/strain-free Si on BPSG was annealed to reach stress balance [7]. The identical strain shift during annealing in the two layers shows that the bilayer remained coherent and dislocations did not play an important role in relaxing the strain.

In this work, instead of growing Si on top of relaxed $Si_{0.70}Ge_{0.30}$, layers with Ge content of 60% have been used. These layers were then coherently relaxed to yield a larger in-plane lattice constant.

EXPERIMENTS AND DISCUSSIONS

A 30-nm commensurately strained $Si_{0.70}Ge_{0.30}$ was transferred to a 1-μm-thick BPSG film by wafer bonding and Smart-cut® processes mentioned earlier. This continuous SiGe film was then pattern into islands (20 μm to 40 μm in edge length), followed by an annealing at 800°C for 30 min to relax the compressive strain. After the strain relaxation of the $Si_{0.70}Ge_{0.30}$ film, an 30-nm epitaxial $Si_{0.4}Ge_{0.6}$ film was deposited using rapid-thermal chemical vapor deposition (RT-CVD) at around 500°C, using dicholorsilane and germane in hydrogen.

Raman spectroscopy was used to locally probe (~ 3 μm resolution) the strain in the SiGe films, using an Ar^+ laser (514.5 nm). The Raman frequency shift of the scattered light due to the optical phonon modes in the SiGe films was measured with an accuracy of ±0.5 cm^{-1}. The phonon energy (and thus Raman shift) depends on the strain level in the films and thus can be used to extract the value of the strain. Because the Si-Si phonon peak in Ge-rich films is typically weak, the position of the Si-Ge phonon peak is used for strain extraction in $Si_{0.4}Ge_{0.6}$ films. The strain $\varepsilon_{Ge=30\%}$ in the $Si_{0.7}Ge_{0.3}$ layer and the strain $\varepsilon_{Ge=60\%}$ in the $Si_{0.4}Ge_{0.6}$ layer were inferred from the optical phonon frequencies ω_{Si-Si} and ω_{Si-Ge} as follows:

$$\omega_{Si-Si}(Si_{0.7}Ge_{0.3}) = 499\ cm^{-1} - 815\varepsilon_{Ge=30\%}\ cm^{-1}\ [8], \quad (2)$$

$$\omega_{Si-Ge}(Si_{0.4}Ge_{0.6}) = 405\ cm^{-1} - 660\varepsilon_{Ge=60\%}\ cm^{-1}\ [9,10]. \quad (3)$$

In the first experiment, a 30-nm $Si_{0.4}Ge_{0.6}$ film was selectively grown on relaxed 30-nm $Si_{0.70}Ge_{0.30}$ islands on BPSG. Raman spectroscopy shows strain of 0.0% in the $Si_{0.70}Ge_{0.30}$ layer and an initial strain ε_0 of –1.1% in the $Si_{0.4}Ge_{0.6}$ layer, in good agreement with that of –1.2% expected from the compositions of the two layers. This sample was then annealed at 800°C for 20 min. Given the thick BPSG and island thickness, the duration of this annealing should be adequate for islands to reach stress balance [6]. As shown in Fig. 2, all phonon peaks from

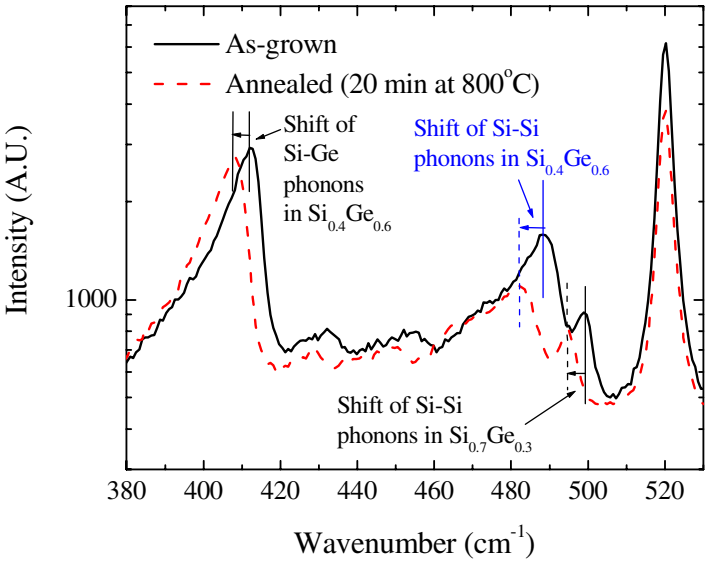

Fig. 2. Raman spectrum, measured at the center of a 20 µm x 20 µm island comprising 30nm $Si_{0.4}Ge_{0.6}$/30nm $Si_{0.7}Ge_{0.3}$, before and after 800°C annealing for 20 min. All phonon peaks from both films shift toward lower wavenumbers after an annealing to reach stress balance, consistent with coherent lateral expansion of the island.

$Si_{0.70}Ge_{0.30}$ and $Si_{0.4}Ge_{0.6}$ films shift toward lower wavenumber upon stress balance, indicating stretching of the films. This is consistent with expected lateral expansion of the $Si_{0.70}Ge_{0.30}$ and $Si_{0.4}Ge_{0.6}$ films. The final strains in the $Si_{0.70}Ge_{0.30}$ and $Si_{0.4}Ge_{0.6}$ layers are 0.55% and –0.50%, respectively. The fact that the strain in both films increased almost identically by about 0.60% indicates that the two layers remained coherent. The strain data from Raman measurement is summarized in Fig. 3. Along with the coherent bilayer condition, Eq. (1) can be used to predict the final strain:

$$\varepsilon_{Ge=30\%} = -\varepsilon_0 \frac{E_{Ge=60\%} h_{Ge=60\%}}{E_{Ge=30\%} h_{Ge=30\%} + E_{Ge=60\%} h_{Ge=60\%}} = 0.54\% \quad (4)$$

$$\varepsilon_{Ge=60\%} = \varepsilon_0 \frac{E_{Ge=30\%} h_{Ge=30\%}}{E_{Ge=30\%} h_{Ge=30\%} + E_{Ge=60\%} h_{Ge=60\%}} = -0.57\% \quad (5)$$

where Possion's ratio is taken to be the same in both films for simplification, and $E_{Ge=30\%}$ and $E_{Ge=60\%}$ are 12.2 x 10^{10} and 11.4 x 10^{10} N/m^2, respectively. Clearly, the stress balance theory accurately predicts the final strain in the films. The in-plane lattice constant of the bilayer at stress balance is equivalent to that of a relaxed $Si_{1-x}Ge_x$ layer with x equal to the average Ge content of this bilayer, which is 45% in this case.

A larger final in-plane lattice constant could in principle be achieved with a thicker $Si_{0.4}Ge_{0.6}$ film or a film of higher Ge content. However, thick layers and/or high Ge content are difficult in practice due to the critical thickness constraint. Alternatively, thinner starting $Si_{0.70}Ge_{0.30}$ layers will lead to a higher average Ge content in the bilayer and thus more relaxation of the $Si_{0.4}Ge_{0.6}$ film and a larger in-plane lattice constant. The dependence of the final strain in the 30-nm $Si_{0.4}Ge_{0.6}$ film on the thickness of the $Si_{0.7}Ge_{0.3}$ layer, based on Eq (5), is plotted in Fig. 4, which also shows the equivalent Ge content of this bilayer. We therefore thinned the original 30-nm fully-relaxed $Si_{0.7}Ge_{0.3}$ layer in a solution of HNO_3:H_2O:HF(0.5%) = 35:20:10 [11], followed by a deposition of the 30-nm $Si_{0.4}Ge_{0.6}$ layer. This bilayer was annealed at 800°C for 20 min to reach stress balance. It is difficult to know the exact thickness of the $Si_{0.7}Ge_{0.3}$ layer

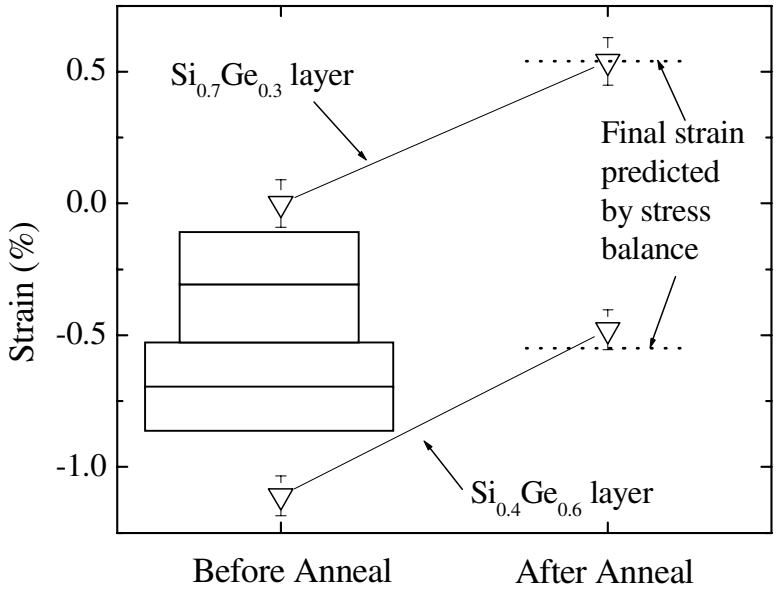

Fig. 3. Biaxial strain of $Si_{0.7}Ge_{0.3}$ and $Si_{0.4}Ge_{0.6}$, measured by Raman spectroscopy at the center of a 20 μm x 20μm island, before and after 20-min annealing at 800°C. Open symbols are experimental data and dotted lines are based on calculation of stress balance.

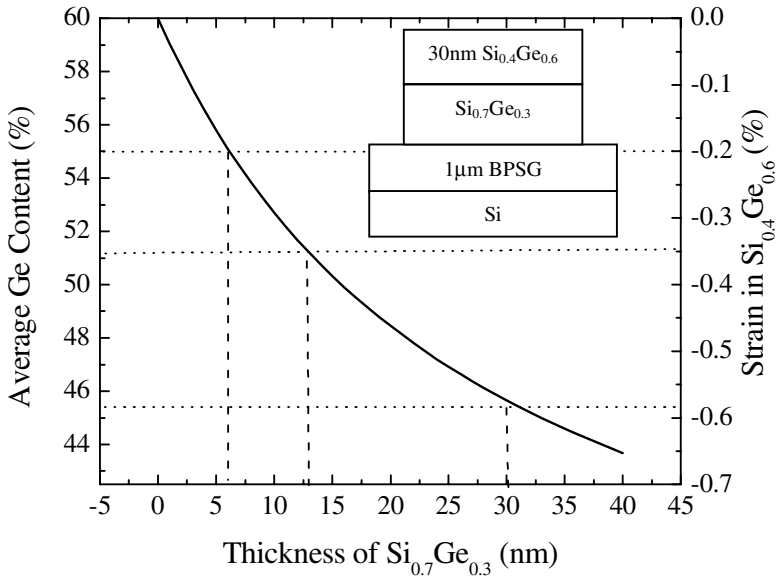

Fig. 4. Average Ge content, predicted by stress balance, as a function of the $Si_{0.7}Ge_{0.3}$ thickness for 30-nm $Si_{0.4}Ge_{0.6}$. Right Y-axis reflects the expected strain in the $Si_{0.4}Ge_{0.6}$ film. The dotted lines show the equivalent Ge content based on the measured strain in the $Si_{0.4}Ge_{0.6}$ and $Si_{0.7}Ge_{0.3}$ films, which is then used to estimate the thickness of the $Si_{0.7}Ge_{0.3}$ film.

after etching because of uncertainty in etch rate, but the thickness can be calculated from the average Ge content of the bilayer, determined by measured final strain in the $Si_{0.4}Ge_{0.6}$ and $Si_{0.7}Ge_{0.3}$ layers, based on Eqs. (4) and (5) (Fig. 4). The equivalent Ge content reached 51% and 55% and the thickness of the final $Si_{0.7}Ge_{0.3}$ layer was 13 nm and 6 nm, respectively (Fig. 4), which shows that this thinning method is very effective in achieving relaxed, high Ge content films.

CONCLUSIONS

Strain relaxation of $Si_{0.4}Ge_{0.6}$ grown on relaxed $Si_{0.7}Ge_{0.3}$/BPSG has been examined and the final strain in the films agrees with stress balance prediction. Both films expand laterally during the annealing, allowing strain relaxation of the $Si_{0.4}Ge_{0.6}$ film without dislocations. Nearly full relaxation of $Si_{0.4}Ge_{0.6}$ is achieved by using a very thin $Si_{0.7}Ge_{0.3}$ film. This shows that the in-plane lattice constant of SiGe films by stress balance on BPSG can be increased to well over 50% and this method is a promising approach for high quality, high Ge content films.

ACKNOWLEDGEMENT

This work is supported by DARPA(N66001-00-10-8957) and ARO(DAAG55-98-1-0270).

REFERENCES:

1. M.L. Lee, C.W. Leitz, Z. Cheng, A.J. Pitera, G. Taraschi, D.A. Antoniadis, and E.A. Fitzgerald, Mat. Res. Soc. Symp. Proc. **686**, pp. A1.9.1-A1.9.5 (2002).
2. J. Welser, J.L. Hoyt, and J.F. Gibbons, IEEE Electron Device Lett. **15**, 100 (1994).
3. S.M. Ting and E.A. Fitzgerald, J. Appl. Phys. **87**, 2618 (2000).
4. E.A. Fitzgerald, Y.-H. Xie, M.L. Green, D. Brasen, A.R. Kortan, and J. Michel, *Appl. Phys. Lett.* **59**, 811 (1991).
5. K.D. Hobart, F.J. Kub, M. Fatemi, M.E. Twigg, P.E. Thompson, T.S. Kuan, and C.K. Inoki, J. Electron. Mater. **29**, 897 (2000).
6. H. Yin, R. Huang, K.D. Hobart, Z. Suo, T.S. Kuan, C.K. Inoki, S.R. Shieh, T.S. Duffy, F.J. Kub, and J.C. Sturm, J. Appl. Phys. **91**, 9716 (2002).
7. H. Yin, K.D. Hobart, F.J. Kub, S.R. Shieh, T.S. Duffy, and J.C. Sturm, to appear in May 26 issue of Appl. Phys. Lett. (2003).
8. J.C. Tsang, P.M. Mooney, F. Dacol, and J.O. Chu, J. Appl. Phys. **75**, 8098 (1994).
9. M.I. Alonso and K. Winer, Phys. Rev. B **39**, 10056 (1989).
10. F. Cerdeira, A. Pinczuk, J.C. Bean, B. Batlogg, and B.A. Wilson, Appl. Phys. Lett. **45**, 1138 (1984).
11. D.J. Godbey, A.H. Krist, K.D. Hobart, and M.E. Twigg, J. Electrochem. Soc. **139**, 2943 (1992).